Characteristic Analysis of CO_2 Switching Arcs under DC current

Xiaoling ZHAO(赵小令)[1], J D Yan[2], Dengming XIAO(肖登明)[1]

[1]Department of Electrical Engineering, Shanghai Jiao Tong University, No.1954 Huashan Rd., Shanghai, 200030, People's Republic of China
[2] Department of Electrical Engineering and Electronics, University of Liverpool, Brownlow Hill, Liverpool L69 3GJ, UK

Abstraction

The current interruption capability of a gas, when used in high voltage gas-blast circuit breakers, depends on not only its material properties but also the flow field since turbulence plays a dominant role in arc cooling during the interruption process. Based on available experimental results, a study of CO_2 Switching Arcs under DC (direct current) current in the model circuit breaker has been conducted to calibrate CO_2 arc model and to analyse its electric and thermal property. Through detailed analysis of the results mechanisms responsible for the temperature distribution are identified and the domain energy transportation process of different region discussed. The present work provides significant coefficients for CO_2 switching arc simulation and gives a better understanding of CO_2 arc burning mechanism.

Keywords: CO_2 switching arc, thermal and electric property, energy transportation.

Some figures may appear in colour only in the online journal.

1 Introduction

Due to its good thermodynamic and transport properties, SF_6 (sulphur hexafluoride) is widely used as an arc interruption medium in circuit breakers and electric switching equipment [1, 2]. However, with the adverse effects on atmosphere and potential facilitation on global warming, SF_6 gas has been listed among the six controlled global warming gases in 1997 according to the Kyoto protocol at COP3 (the 3rd Conference of Parties) [3]. CO_2 gas has a superior dielectric strength[4] and thermal interruption performance [5], and attracts the attention of researchers as an arc-extinguishing medium for circuit breakers [6]. To evaluate the interruption capability and the arc extinguishing mechanism of a gaseous medium, establishing a theoretical model of switching arcs is of great importance in identifying the dominant energy transport process responsible for the arc characteristics.

Researchers have long been on the way to build up suitable computational models for different gases in arc extinguishing processes. As early as 1990s, M T C Fang and Q Zhuang has utilized laminar flow [7] and turbulent flow [8] based on local thermal equilibrium to study the current-zero behaviour of an SF_6 gas-blast arc. J D Yan et al. compared the two most popular turbulence models, the Prandtl mixing length model and the *k*-ε model, for SF_6 arcs in a supersonic nozzle [9]. Recently, J Liu et al. utilized Laminar flow, Prandtl mixing length model and modified *k*-ε turbulence to simulate an air arc burning in a supersonic nozzle and obtain a satisfactory turbulence model for air arcs[10]. CO_2 gas is a significant medium either as a puffer gas mixed with other gases or a potential substitute of SF_6 in switchgear equipment. Although a lot of work related to the CO_2 plasma modelling have been published recently[11-14], there is few literatures that could give satisfactory arc model for CO_2 in switching application.

In the present study, we use modified *k*-ε turbulence model to build up CO_2 switching arc model under DC (direct current) current in model HV circuit breaker, trying to find out proper turbulence and radiation coefficients to accurately predict the radical temperature profile at high temperature. The results will facilitate the CO_2 arc theoretical study afterwards and provides significant accordance for CO_2 arc simulation. Then the physical mechanisms and its relationship with thermodynamic properties are explored through the detailed analysis of the model results. Good understandings of CO_2 switching arc can help assess the arc interruption capability and design suitable structure for switchgear apparatus.

2 Arc model frameworks

2.1 Governing equations

The computer simulation of the switching arc model is based on the solution of a series of conservation equations. The governing equations are modified from Navier-Stokes equations [15] to take Lorentz force, Ohmic heating and radiation into considerations as momentum source and energy source [16, 17].

The mass conservation equation is expressed as

$$\frac{\partial \rho}{\partial t} + \nabla \cdot \left(\rho \boldsymbol{V} \right) = 0 \tag{1}$$

Where ρ is the density, t is the time, $\boldsymbol{V}$ is the velocity vector.

The momentum conservation equation is expressed as

$$\frac{\partial}{\partial t}\left(\rho \boldsymbol{V}\right)+\nabla\cdot\left(\rho \boldsymbol{V}\boldsymbol{V}\right)=-\nabla p+\nabla\cdot\overline{\overline{\tau}}+\boldsymbol{J}\times\boldsymbol{B} \tag{2}$$

Where p is the pressure, $\overline{\overline{\tau}}$ is the stress tensor, $\boldsymbol{J}$ is the current density vector and $\boldsymbol{B}$ is the magnetic flux density.

The energy conservation equation is expressed as

$$\frac{\partial}{\partial t}\left(\rho e\right)+\nabla\cdot\left(\boldsymbol{V}\left(\rho e+p\right)\right)=\nabla\cdot\left(k\nabla T+\overline{\overline{\tau}}\cdot\boldsymbol{V}\right)+\sigma\boldsymbol{E}^{2}-q \tag{3}$$

Where k is thermal conductivity, σ is electric conductivity, $\boldsymbol{E}$ is the electric field strength and q is the net radiation loss. In equation (3), e is a parameter relates to enthalpy h expressed as

$$e=h-\frac{p}{\rho}+\frac{V^{2}}{2} \tag{4}$$

In equation (2) and (3), the stress tensor $\overline{\overline{\tau}}$ is given by

$$\overline{\overline{\tau}}=\left(\mu_{l}+\mu_{t}\right)\left[\left(\nabla\boldsymbol{V}+\nabla\boldsymbol{V}^{T}\right)-\frac{2}{3}\nabla\cdot\boldsymbol{V}\boldsymbol{I}\right] \tag{5}$$

Where μ_l and μ_t is respectively laminar and turbulent viscosity, and $\boldsymbol{I}$ is a unite identity matrix. For laminar flow model, μ_t=0.

The expression of electric potential in Maxwell's equations is used to calculate the electric voltage distribution in space, which can be also regard as conservation equation for electric charge, expressed as

$$\nabla\cdot\left(-\sigma\nabla\varphi\right)=0 \tag{6}$$

Where φ is electric potential, σ is electric conductivity. Then electric field $\boldsymbol{E}$ strength is expressed as the special gradient of electric potential

$$\boldsymbol{E}=-\nabla\varphi \tag{7}$$

With the electric field and conductivity distribution, the energy input in arc coming from Ohmic heating is described in arc model, and can be take into the energy transport equation as energy source in equation (3). The calculation in the present paper is based on the thermodynamic and transport parameters of CO_2 [18, 19] at high temperature and pressure.

2.2 Flow model

The laminar flow is smooth and the adjacent layers in fluid slide past each other in an orderly fashion. With laminar flow, only the mass, momentum and energy conservation equations with extra sources are solved. For turbulence flow, the flow behaviour is random and chaotic with varied velocity and all other flow properties. A reliable model to describe the random nature of a turbulence flow is *k*-*ε* model, which adds two extra partial differential equations to compute the length and velocity scales of turbulence, and finally the eddy viscosity. One equation is for the turbulent kinetic energy per unit mass *k*, while the other for the turbulence dissipation rate *ε*, which are given as

$$\frac{\partial}{\partial t}(\rho k)+\nabla\cdot(\rho k\boldsymbol{V})=\nabla\cdot\left(\left(\mu_l+\frac{\mu_t}{\sigma_k}\right)\nabla k\right)+G_k-\rho\varepsilon \tag{8}$$

$$\frac{\partial}{\partial t}(\rho\varepsilon)+\nabla\cdot(\rho\varepsilon\boldsymbol{V})=\nabla\cdot\left(\left(\mu_l+\frac{\mu_t}{\sigma_k}\right)\nabla\varepsilon\right)+G_{1\varepsilon}G_k\frac{\varepsilon}{k}+G_{2\varepsilon}\rho\frac{\varepsilon^2}{k} \tag{9}$$

In an axisymmetric geometry, the generation rate of the turbulence kinetic energy G_k is expressed by

$$G_k=\mu_t\left(2\left(\frac{\partial w}{\partial z}\right)^2+2\left(\frac{\partial v}{\partial r}\right)^2+2\left(\frac{v}{r}\right)^2+\left(\frac{\partial w}{\partial r}+\frac{\partial v}{\partial z}\right)^2\right) \tag{10}$$

Where *w* and *v* are respectively velocity on the axial and radial direction, *z* and *r* are axial and radial coordinates. The expression of the length, velocity and eddy viscosity are

$$\lambda_c=C_u\frac{k^{1.5}}{\varepsilon} \tag{11}$$

$$V_c=\sqrt{k} \tag{12}$$

$$\mu_t=\rho C_u\frac{k^2}{\varepsilon} \tag{13}$$

In standard *k*-ε model, the model constants[15] are:

$$G_{1\varepsilon}=1.44, G_{2\varepsilon}=1.92, G_\mu=0.09, \sigma_k=1.0, \sigma_\varepsilon=1.3$$

Such default values are determined in consideration of common shear flows including boundary layers, mixing layers and jets, and work well for most free shear flows. However, as a complicated turbulence model with both high temperature and pressure, some of them may need justification to better satisfy a certain gas arc.

2.3 Radiation model

As switching arc is thermal plasma in high pressure condition, whose temperature profile is affected not only by the flow, but also by radiation. In the energy conservation equation, energy source includes Ohmic heating and radiation source, both of which play an important role in the distribution of temperature and its distribution. Radiation loss is expressed as

$$e_{tr} = -\int_{z_1}^{z_2}\left(\int_0^R q 2\pi r \mathrm{d}r\right)\mathrm{d}z \tag{14}$$

Where e_{tr} is transparent radiation, q is the emission coefficient. R is radiation radius which is the average of arc core boundary and arc boundary. (Z_1-Z_2) is the arc length, i.e. the distance between two electrodes.

Arc radiation model based on net emission coefficient (NEC) is a semi-empiricism model introduced by Zhang J F et. al. The approximate NEC is defined as the net emission coefficient on the axis of an isothermal plasma cylinder, which depends on the temperature, pressure and the radius of the cylinder. It is noted that these radius and factors such as the multiplying factor and percentage of radiation leaving the core boundary, which is re-absorbed, are not fixed but can be adjusted[20]. The magnitude of NEC directly affects the temperature of the core area, while the percentage of reabsorption has an obvious influence on the arc radius. The higher the absorbed percentage, the larger the arc radius.

2.4 Computational geometry and boundary conditions

The present computation is based on the CO_2 switching arc experiments of literature[21, 22] using ANSYS 17.0 Fluent solver. The computation domain and the grid system in an asymmetrical geometry are shown in figure 1, where HV and GND represent the contacts connecting to high voltage electric source and ground respectively. Tests for different meshing size have been made to suppress the effect from the grid on the simulation accuracy. The domain includes two nozzles and two fixed contact with an inlet and an outlet. The computation domain is divided into 4 zones. Arc burning area is meshed by structured grids (uniform rectangular grids), and the rest non-structured grids.

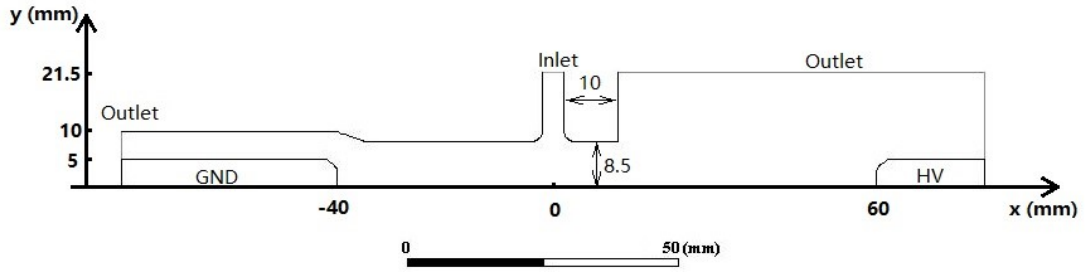

Figure 1. Nozzle geometry and grid system (unite: mm).

The input current from outside circuit is 1 kA DC. The roles of Ohmic heating, radiation and Lorentz force are all taken into consideration as momentum and energy source in the governing equations. The boundary conditions for the inlet and outlet is set to be 350,000 Pa and 0 as relative pressure to atmosphere pressure, according to the experiment process described in literature [21]. A more detailed list of boundary conditions is shown in table 1. An arc column of uniformly varying temperature is set near the axis of the geometry as initial conditions of arc with central temperature of 15 kK decreasing to 300 K at radius of 1.5 mm. A UDS (user-defined scalar) is adopted to solve partial differential equation for electric potential, whose boundary conditions are set as flux value of 1000 A at high-voltage contact and 0 V at a ground contact.

Table 1. Boundary conditions in CO_2 switching arc model

Boundary	Boundary Conditions
Axis	0 for axial component of variables (except velocity) of control equations
Inlet	350,000 Pa for pressure
Outlet	0 for pressure
HV contact	1000 A for arc current
GND contact	0 V for voltage
Other solid surface	non-slip walls for velocity, 0 for heat conductivity

3 The calibration of CO_2 switching arc model

Previous investigation have been conducted on SF_6 [23-25] and air [10] switching arc models based on Navier-Stokes equations with suitable radiation and turbulence model. As a potential arc interruption medium or even a puffer gas in switchgear apparatus, the fluid-arc model for CO_2 gas, which is of great importance in studying CO_2 arc mechanism, has not been calibrated or set up in published literatures yet. In this section, we firstly analysis the influence of radiation and turbulence coefficients, and then calibrate the model by comparing the calculated radial temperature profile with the spectroscopically measured value [21].

3.1 The effect from radiation coefficients

The NEC radiation model has been applied to simulate the radiation effect of arcs in different conditions and physical structures. Based on these successful cases, Dixon [20]pointed out that some coefficients in NEC model need to be changed to adopt different working gases and conditions, including the identification of radiation radius, radiation loss coefficient and re-absorption coefficient. For example of SF_6 arc, Yan[9] make the radiation coefficient as the NEC value obtained by Liebermann[26] multiplied by 2.5 in arc core area, while Kwan[27] make it as a multiplication ratio, and Fang[7, 8] make it multiplied by 1.5.

The radial temperature profile measured by is at the stagnation point at nozzle upstream. In the model geometry built in figure 1, the velocity profile on axis is shown in figure 2. It is clear that the observation point is at the axial coordinate of -1.5 mm and the radial temperature at this point is traced to calibrate CO_2 switching arc model.

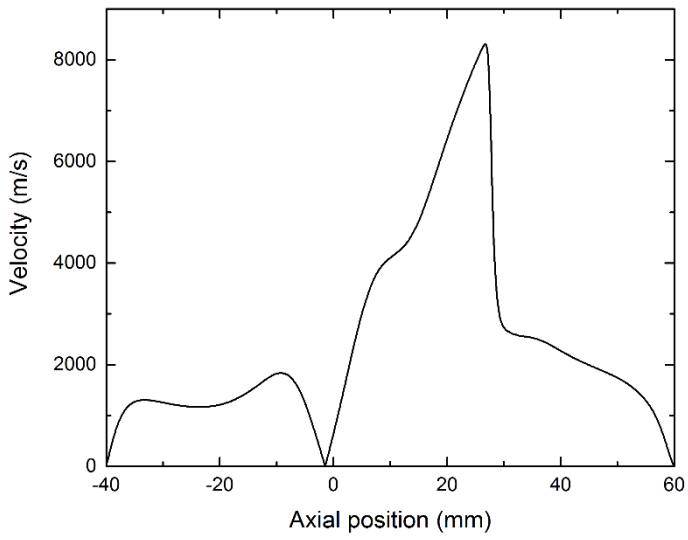

Figure 2. Arc Velocity profile in the axial direction

Fixed re-absorption coefficient as 0.8, the CO_2 arc models are set up with radiation loss coefficient from 1.0 to 3.0. The calculated radial temperature profiles with different radiation loss coefficient are shown in figure 3. Seen from the result, the radiation loss coefficient mainly affects the arc temperature distribution in core region with relatively small effect on re-absorption region. The higher the radiation loss coefficient, the more the energy loss by the way of radiation, and the lower the temperature in arc core region is. Oppositely the temperature outside the arc core will

slightly increase with this coefficient. Its influence on the arc temperature becomes weaker with the increasing radiation loss coefficient.

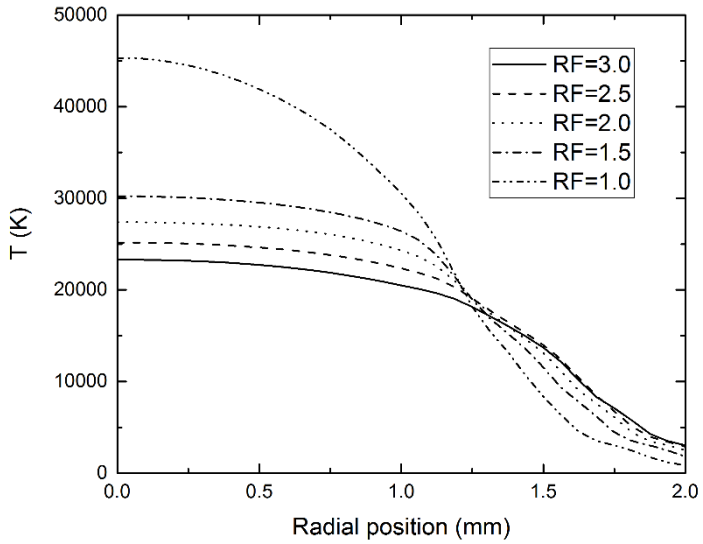

Figure 3. The effect of radiation calibration coefficient on the arc radial temperature profile

Fixed the radiation loss coefficient at 2.5, the CO_2 switching arc models are set up with different re-absorption coefficient with radial temperature shown in figure 4. With re-absorption coefficient increasing from 0.5 to 0.8, the temperature and radius become larger and the changing rate of temperature affected by coefficient become stronger. Despite of application in radiation absorption region, the temperature at arc core are also influenced by re-absorption coefficient. Generally speaking, the arc temperature is more sensitive of the radiation loss coefficient than of the re-absorption one.

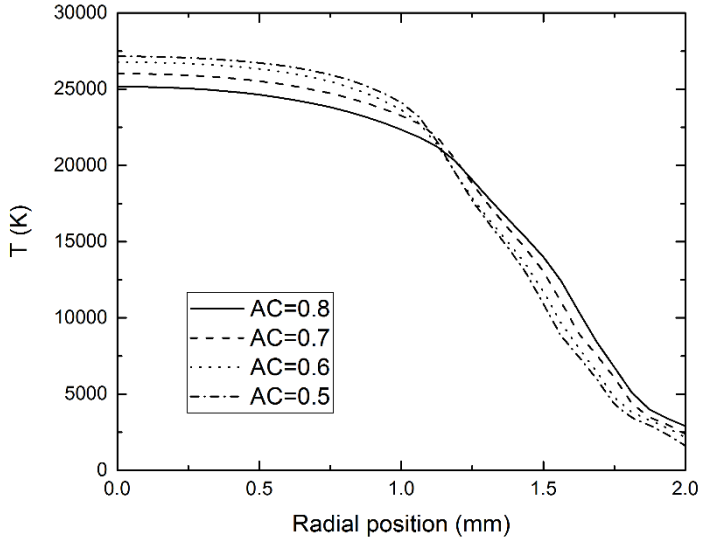

Figure 4. The effect of re-absorption coefficient on the arc radial temperature profile

3.2 The effect from turbulence coefficient

For different gaseous medium in different conditions, the strength of turbulent effect is also different. Early researchers used laminar model to simulate nitrogen gas arc and obtained satisfactory results[28]. However, when applied to SF_6 gas blowing arc, the calculation result diverged greatly from the experiments[7]. Thus, CO_2 switching arc model also need appropriate turbulent strength to give sufficiently accurate calculation.

Among different constants in k-ε model, $C_{1\varepsilon}$ can be adapted to simulate different strength of turbulence effect[9]. The higher the value, the weaker the turbulence effect. When fixing radiation loss coefficient as 3.0 and re-absorption coefficient as 0.8, the radial temperature profiles are calculated with different $C_{1\varepsilon}$ values, shown in figure 5. Seen from the result, turbulence effect will have obvious effect on both the arc temperature and radius. With stronger turbulence, the central temperature becomes lower, and arc radius becomes smaller. Because turbulence intensifies the energy transportation process and help cooling down arc.

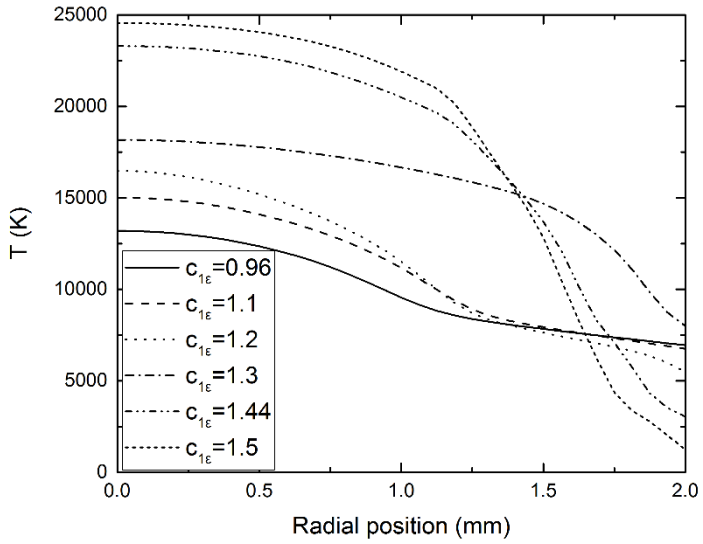

Figure 5. The effect of turbulent intensity on the arc radial temperature profile

3.3 The calibration of CO_2 switching arc model

With analysis of the influence of different coefficients, the radial temperature profiles with potential suitable radiation and turbulence models are calculated. The results are compared to the arc temperatures profile obtained by spectroscopic Measurements in a model circuit breaker [21] in figure 6. When radiation loss coefficient is 3.0, re-absorption one is 0.8 and the value of $C_{1\varepsilon}$ is 1.38, the radial temperature at upstream stagnation point corresponds to that of experiment with derivation within test error, which could be regarded as suitable model.

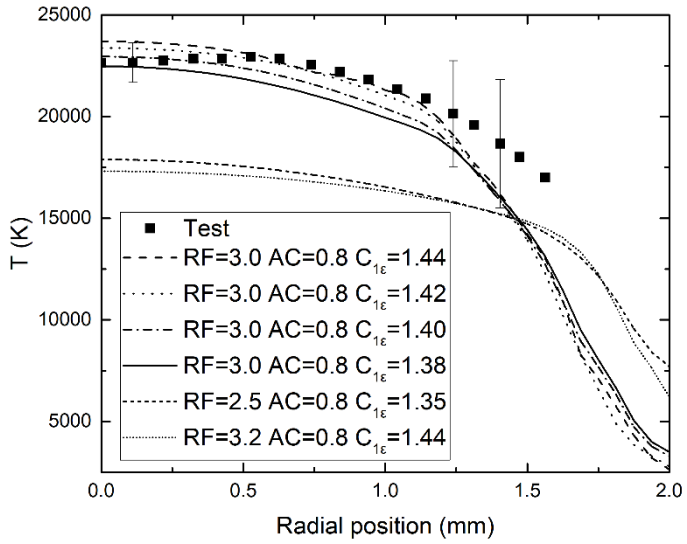

Figure 6. The comparison of the arc radial temperature profiles between computational and measured values

4 Results and Discussion

The fluid and arc conservation equations based on *k*-ε turbulence model have been solved for DC current at a stagnation pressure of 3.5 bar at upstream. The computed results of radial temperature profiles are in good agreement with the experimental ones.

4.1 General thermal and electric properties of CO_2 arc

The temperature distribution during arc burning process determines the local electric conductivity, and are affected by flow field around. The spatial distribution of temperature at 1 kA is shown in figure 7, with the maximum temperature of 25850 K and small radius of 1.85 mm at throat of main nozzle. For the both the two nozzles, the radius at upstream is smaller than that at downstream with higher temperature. The arc in main nozzle is slimmer than that in auxiliary nozzle.

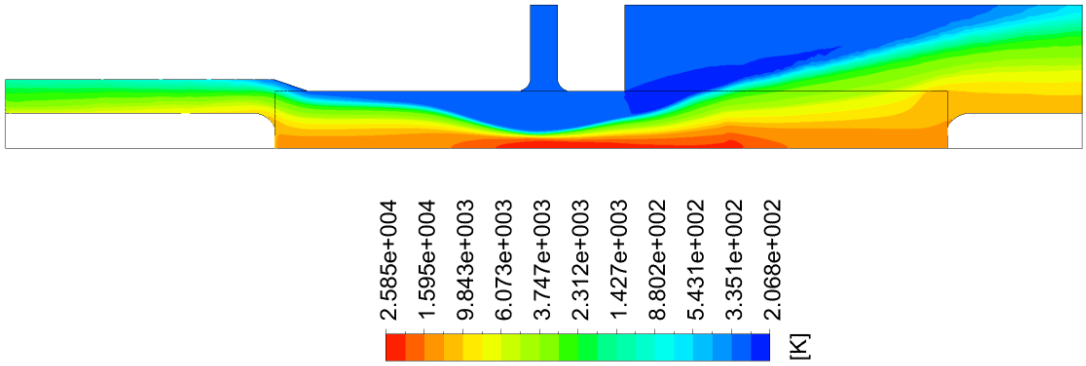

Figure 7. The temperature distribution contour of switching arc model

In nozzle structure, gas will be accelerated from convergent to divergent space, which improves the efficiency of energy transportation in arc and helps cool off arc. The flow velocity and Mach number of gas in nozzle are shown in figure 8. The flow coming from inlet starts to accelerate from the stagnation point and reach the maximum velocity at downstream. For main nozzle on the right, the divergent angle is as large as 90°, and the gas velocity at downstream is beyond sound velocity (Mach number >1). The main nozzle is a supersonic nozzle, where the velocity is sound speed at nozzle throat and exceeds it at divergent area. On the other hand, the auxiliary nozzle is a subsonic nozzle. So, the main nozzle has stronger effect on arc which has smaller radius and higher central temperature. The velocity is mainly determined by local pressure gradient, and the relative pressure contour in the nozzles is shown in figure 9. It can be seen that the pressure at downstream of main

nozzle is even below the atmosphere pressure. The large pressure gradient distributed in main nozzle explains the supersonic speed appeared.

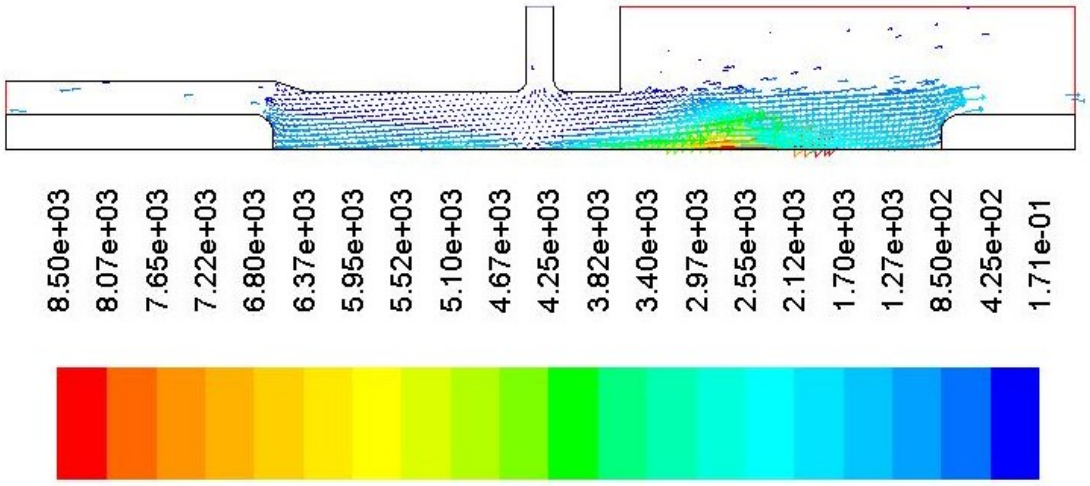

(a) velocity（unite：m/s）

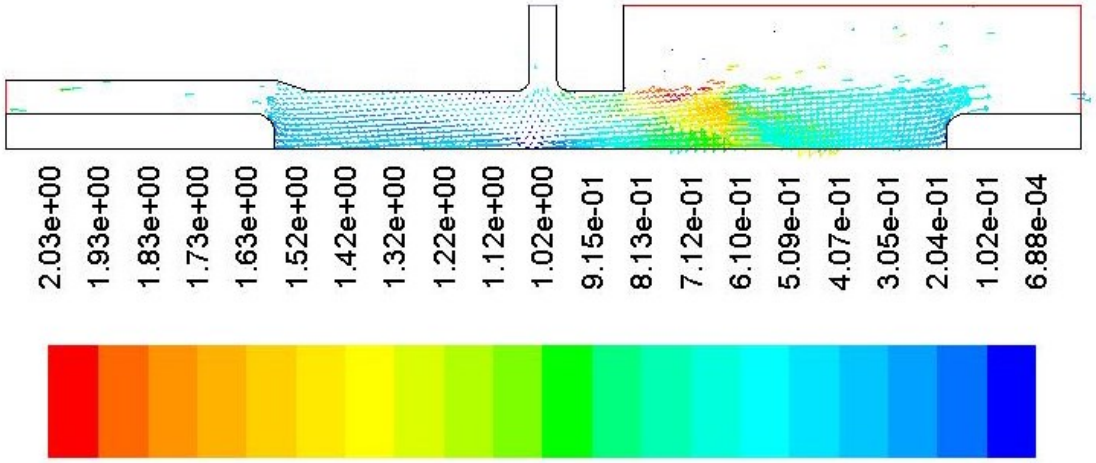

(b) Mach number

Figure 8. The velocity vectors in the switching arc model

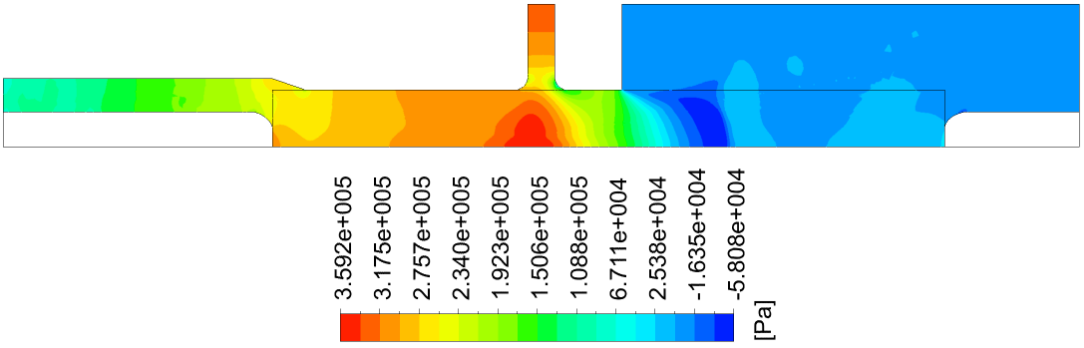

Figure 9. The gas pressure distribution in the switching arc model (The negative value means a pressure below atmosphere pressure.)

The electric conductivity of thermal arc plasma is determined by temperature, and further affect electric potential distribution. The potential gradient, i.e. electric field strength, in plasma with high electric conductivity will generate Ohmic heating and improve the arc temperature. Figure 10 gives the electric potential contour with arc voltage of 527 V. The electric potential changes fast near nozzle throat in space and generate large electric field strength. This explains the phenomenon that the arc temperature reaches the maximum at throat (see figure 7).

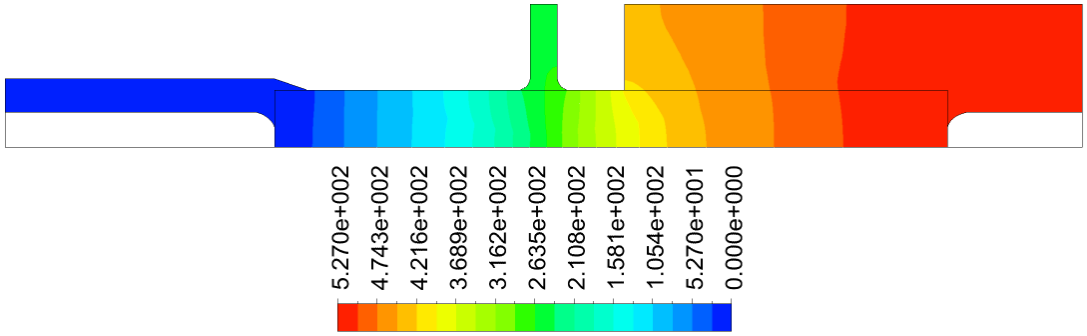

Figure 10. The arc voltage distribution in the switching arc model (unite: V)

According to Maxwell's equation, changing electric field will produce magnetic field. The interaction between electric and magnetic fields will generate Lorentz force and have an arc clutch effect to make arc slim. The magnetic induction strength contour is shown in figure 11, which is closely related to current density. The strong Lorentz force at throat further decrease arc radius. In the two-dimension structure with axial symmetry, the negative value of magnetic induction strength means its directions pointing in the displaying surface, thus the direction of Lorentz force is to the axis for an electron according to right-hand grip rule.

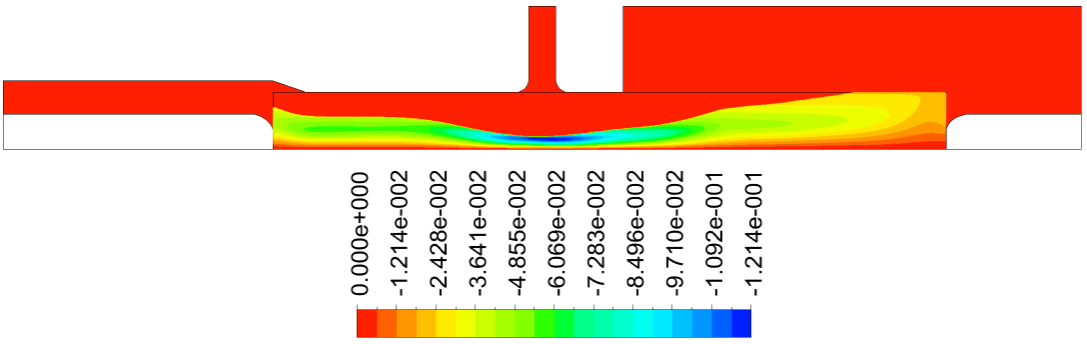

Figure 11. Magnetic induction strength contour (unite: B)

4.2 Energy balance analysis

In arc plasma, the input energy from Ohmic heating will be transport outwards through different processes. And the energy generation and loss efficiency determine the thermal and electric property of an arc. We make energy balance analysis at arc core boundary (at radius of 83% of the maximum radial temperature) and electric boundary (at radius of 4000 K), and the Ohmic heating input energy as well as ratio of each energy transport form and input energy are listed in table 2, where positive value means energy input and negative means energy loss.

In arc core region and electric region, the expressions of various energy transport processes are listed below as

$$\text{Ohmic heating} = \int_{z_1}^{z_2}\left(\int_0^R \sigma E^2 2\pi r \mathrm{d}r\right)\mathrm{d}z \tag{15}$$

$$\text{Radiation loss} = \int_{z_1}^{z_2}\left(\int_0^R q 2\pi r \mathrm{d}r\right)\mathrm{d}z \tag{16}$$

$$\text{Radial conductivity} = \int_{z_1}^{z_2}\left(\int_0^R \frac{1}{r}\frac{\partial}{\partial r}\left(rk\frac{\partial T}{\partial r}\right)2\pi r \mathrm{d}r\right)\mathrm{d}z \tag{17}$$

$$\text{Axial convection} = -\int_{z_1}^{z_2}\left(\int_0^R \rho v\frac{\partial h}{\partial z}2\pi r \mathrm{d}r\right)\mathrm{d}z \tag{18}$$

$$\text{Radial convection} = -\int_{z_1}^{z_2}\left(\int_0^R \rho w\frac{\partial h}{\partial r}2\pi r \mathrm{d}r\right)\mathrm{d}z \tag{19}$$

$$\text{Pressure work} = \int_{z_1}^{z_2}\left(\int_0^R \frac{\partial p}{\partial t}2\pi r \mathrm{d}r\right)\mathrm{d}z \tag{20}$$

Where R is radial integral boundary which is radius at 83% of maximum temperature for arc core and radius at 4000 K for electric region, Z_2 and Z_1 is respectively axial integral boundary which is the coordinate of two arc ends. The pressure work is neglected as the percentage in energy input below 5%.

Table 2. Electric energy input and different energy transport processes at arc core and electric boundary

Arc Boundary	Energy input	Radiation loss	Radial conductivity	Axial convection	Radial convection
Core boundary	275564.2 W	-57.67%	-59.75%	41.65%	-27.44%
Electric boundary	566948.9 W	-11.89%	-76.04%	5.35%	-24.89%

At arc core boundary, radiation and radial conductivity play the major roles in energy transportation. Axial convection is in fact an energy generation process. Because the directions of

spatial enthalpy increase and the axial velocity are the opposite in this specific nozzle structure, seen from figure 7 and 8. At electric boundary, 80% radiation emitted from arc core is re-absorbed into the arc, thus the radiation loss reduced to 12% of the energy input. Radial conductivity become the domain energy transport form.

5 Conclusion

The recent work built up a computational switching arc model for CO_2 gas to study its thermal and electric features. By compared the calculated radial temperature profile with the measured, we calibrated the radiation and turbulence model with satisfactory result within the test error.

The main conclusions are listed below.

（1） For CO_2 switching arc model, the proper radiation loss and re-absorption coefficient are respectively 3.0 and 0.8, and the value of $C_{1\varepsilon}$ is 1.38. This work facilitates the CO_2 arc theoretical study and provides significant accordance for subsequent arc simulation exploration.

（2） At 1 kA DC current, the accelerated flow in nozzle and CO_2 arc interact with each other and together affect the temperature distribution of arc plasma. The maximum temperature appears at nozzle throat with strong electric field strength and high electric conductivity. The arc radius becomes larger at downstream.

（3） As for energy transportation, the domain process of CO_2 switching arc is radiation and radial conductivity together at core boundary, and is radial conductivity at electric boundary.

Acknowledgments

This work is supported by National Natural Science Foundation of China (Grant No. 51337006).

Reference:

[1] Christophorous L G, Olthoff J K 1998 *Gaseous Dielectrics VIII*
[2] Wang W Z *et al* 2013 *J. Phys. D: Appl. Phys.* **46** 065203
[3] Dervos C T and Vassiliou P 2000 *J. Air Waste Manage. Assoc.* **50** 137
[4] Colombo V, Ghedini E and Sanibondi P 2011 *Plasma Sources Sci. Technol.* **20** 035003
[5] Uchii T *et al* 2004 *IEEJ Trans. Power Energy* **124** 469
[6] Udagawa K *et al* 2011 *International Conference on Power Systems Transients* **62271** 100
[7] Fang M T C and Zhuang Q 1992 *J. Phys. D: Appl. Phys.* **25** 1197
[8] Fang M T C, Zhuang Q and Guo X J 1994 *J. Phys. D: Appl. Phys.* **27** 74
[9] Yan J D, Nuttall K and Fang M T C 1999 *J. Phys. D: Appl. Phys.* **32** 1401
[10] Liu J *et al* 2016 *J. Phys. D: Appl. Phys.* **49** 435201

[11] Wang W Z *et al* 2016 *Plasma Sources Sci. Technol.* **25** 065012
[12] Wang W Z *et al* 2017 *Chem. Eng. J.* **330** 11
[13] Wang W Z and Bogaerts A 2016 *Plasma Sources Sci. Technol.* **25** 055025
[14] Zhao X L, Jiao J T and Xiao D M 2016 *Plasma Sci. Technol.* **18** 1095
[15] Versteeg H K and Malalasekera W 2007 *An Introduction to Computational Fluid Dynamics: The Finite Volume Method* (Harlow: Prentice Hall)
[16] Yan J D. 1997, Investigation of electric arcs in self-generated flow. Ph.D thesis, University of Liverpool
[17] Lythall R T 1972 *The J. & P. Switchgear Book: An Outline of Modern Switchgear Practice for the Non-Specialist User* (Newnes-Butterworths)
[18] Tanaka Y, Yamachi N and Matsumoto S, *et al* 2006 *IEEJ Transactions on Power and Energy.* **126** 80
[19] Matsumura T, *et al* 2009 *Proc. of The Seventh Int. Symp. on Applied Plasma Science* 59
[20] Dixon C M, Yan J D and Fang M T C 2004 *J. Phys. D: Appl. Phys.* **37** 3309
[21] Methling R, Franke S and Uhrlandt D 2015 *Plasma Phys. Technol.* **2** 290
[22] Stoller P C *et al* 2014 *J. Phys. D: Appl. Phys.* **48** 015501
[23] Wang W. 2013, Investigation of the dynamic characteristics and decaying behaviour of SF_6 Arcs in switching applications. Ph.D thesis, University of Liverpool
[24] Zhang Q, Yan J D and Fang M T C 2013 *J. Phys. D: Appl. Phys.* **46** 165203
[25] Wang W Z *et al* 2017 *J. Phys. D: Appl. Phys.* **50** 074005
[26] Liebermann R W and Lowke J J 1976 *J. Quantit. Spectrosc. Radiat. Transfer* **16** 253
[27] Kwan S. 1996, Computer simulation of arcs in gas-blast circuit-breakers. Ph.D thesis, University of Liverpool
[28] Zhang J F, Fang M T C and Newland D B 1987 *J. Phys. D: Appl. Phys.* **20** 368